The Multiphase Nature of the Cu(pz) and Ag(pz) (Hpz = Pyrazole) Systems: Selective Syntheses and *Ab-Initio* X-ray Powder Diffraction Structural Characterization of Copper(I) and Silver(I) Pyrazolates

Norberto Masciocchi,*,† Massimo Moret,† Paolo Cairati,† Angelo Sironi,*,† G. Attilio Ardizzoia,‡ and Girolamo La Monica‡

Contribution from the Istituto di Chimica Strutturistica Inorganica and Dipartimento di Chimica Inorganica, Metallorganica ed Analitica, Università di Milano and Centro CNR via Venezian 21, I20133 Milano, Italy

Received January 10, 1994®

Abstract: Copper(I) and silver(I) pyrazolates, depending on the synthetic method used, appear in two distinct crystalline phases each. The crystal and molecular structures of the polymeric α-$[Cu(pz)]_n$ and $[Ag(pz)]_n$ and of the trimeric $[Ag(pz)]_3$ complexes (Hpz = pyrazole) have been determined *ab-initio* using X-ray powder difrraction data from conventional laboratory equipment and refined with the Rietveld technique. Crystals of α-$[Cu(pz)]_n$ are orthorhombic, space group *Pbca* (no. 61), with a = 6.6684(4) Å, b = 19.829(1) Å, c = 6.0847(4) Å, and Z = 8; $[Ag(pz)]_n$ crystallizes in the orthorhombic space group *Pbca* (no. 61) with a = 6.5295(4) Å, b = 20.059(2) Å, c = 6.4675(4) Å, and Z = 8. A 1:1 mixed metal phase, $[(Cu,Ag)(Pz)]_n$, has also been prepared which shows high crystallinity with lattice parameters intermediate between those of the pure Cu and Ag phases. $[Ag(pz)]_3$ crystallizes in the orthorhombic space group *Pbcn* (no. 60) with a = 13.147(1) Å, b = 10.570(1) Å, c = 8.792(1) Å, and Z = 4. For sake of comparison, the crystal structure of the polymeric β-$[Cu(pz)]_n$ phase has also been refined from X-ray powder diffraction data, using prior knowledge from a single crystal X-ray determination. Crystals of β-$[Cu(pz)]_n$ are orthorhombic, space group *Pbcn* (no. 60), with a = 9.933(2) Å, b = 13.348(2) Å, c = 5.954(1) Å, and Z = 8. All four polymeric complexes consist of infinite chains of linearly coordinated copper or silver atoms, bridged by bidentate pyrazolato anions, running parallel to the crystallographic c directions. As a result, the α-$[Cu(pz)]_n$ and β-$[Cu(pz)]_n$ phases differ mainly in the interchain Cu···Cu contacts, which are as low as 2.972(6) Å in the β phase, and in the crystal packing of the polymeric chains. Of the two silver phases, $[Ag(pz)]_n$ is isostructural with α-$[Cu(pz)]_n$, while $[Ag(pz)]_3$ is a trimeric complex of idealized D_{3h} symmetry, topologically similar to that already reported for the 3,5-diphenyl derivative.

Introduction

In the last few years there has been a significant renaissance of powder diffraction (PD) methods which has captured the interest of several groups in the fields of physical, chemical, earth, and, above all, material sciences.[1] Thanks to the widespread availability of advanced high-resolution equipment and intense radiation sources (synchrotrons and time-of-flight neutrons) and to the development of new numerical techniques and algorithms for handling fully digitized spectra, powder diffraction methods are now a powerful tool in the hands of the solid-state scientist.

The recent reports of *ab-initio* structural solutions (and subsequent refinements) of *molecular* organic and metallorganic crystal structures from high-resolution synchronton data first,[2] but lately also from conventional equipment,[3] have prompted us to investigate the possibility of solving simple structures in the field of polymeric metallorganic materials, which usually appear as fine powdered samples; for this class of compounds, single crystals cannot be grown because their negligible solubility in all common solvents prevents the effectiveness of the slow diffusion, gel permeation, or evaporation techniques; in addition, their thermal instability rules out any crystallization process from the melt. Analogously, organic polymers have been extensively studied *via* X-ray PD techniques and several crystal structures successfully refined.[4]

We have recently shown[5] that, using accurate digitized spectra from a conventional diffractometer and up-to-date software, it is possible to obtain useful stereochemical information (local geometry and crystal packing) even from the intrinsically entangled X-ray PD data of $[HgRu(CO)_4]_4$[5a] and polymeric $[Ru(CO)_4]_n$.[5b] In addition, a recent report on the structural determination of polymeric $Cu(SCH_3)$ has appeared in the literature.[6]

Group 11 metals form binary compounds with the deprotonated forms of several pyrazoles (Hpz*) of the general formula $[M(pz^*)_m]_n$ (M = Cu, m = 1, 2; M = Ag, Au, m = 1). Interestingly, the few structurally characterized systems have been found to possess a variety of stoichiometries, molecular arrangements, and oligomeric or polymeric structures.[7] In a few cases, oligomers of different nuclearities have been selectively

† Istituto di Chimica Strutturistica Inorganica.
‡ Dipartimento di Chimica Inorganica, Metallorganica, ed Analitica.
® Abstract published in *Advance ACS Abstracts*, July 1, 1994.

(1) See, for example: *Reviews in Mineralogy*; Bish, D. L., Post, J. E., Eds.; The Mineralogical Society of America: Washington, DC, 1990; Vol. 20.

(2) Cernik, R. J.; Cheetham, A. K.; Prout, C. K.; Watkin, D. J.; Wilkinson, A. P.; Willis, B. T. M. *J. Appl. Crystallogr.* **1991**, *24*, 222. Weiss, E.; Corbelin, S.; Cockroft, J. K.; Fitch, A. N. *Angew. Chem., Int. Ed. Engl.* **1990**, *29*, 650. Honda, K.; Goto, M.; Kurahashi, M. *Chem. Lett.* **1990**, 13. Kurahashi, M. *J. Crystallogr. Soc. Jpn.* **1992**, *34*, 157.

(3) Lightfoot, P. L.; Glidewell, C.; Bruce, P. G. *J. Mater. Chem.* **1992**, *2*, 361. Lightfoot, P.; Tremayne, M.; Harris, K. D. M.; Bruce, P. G. *J. Chem. Soc., Chem. Commun.* **1992**, 1012. Tremayne, M.; Lightfood, P.; Mehta, M. A.; Bruce, P. G.; Harris, K. D. M.; Shankland, K.; Gilmore, C. J.; Bricogne, G. *J. Solid State Chem.* **1992**, *100*, 191. Petit, S.; Coquerel, G.; Perez, G.; Louer, D.; Louer, M. *New J. Chem.* **1993**, *17*, 187. Petit, S.; Coquerel, G.; Perez, G.; Louer, D.; Louer, M. *Chem. Mater.* **1994**, *6*, 116.

(4) See, for example: Hay, J. N.; Kemmish, D. J.; Langford, J. I.; Rae, A. I. M.; *Polym. Commun.* **1984**, *25*, 175; **1985**, *26*, 283. Bruckner, S.; Meille, S. V.; Malpezzi, L.; Cesaro, A.; Navarini, L.; Tombolini, R. *Macromolecules* **1988**, *21*, 967 and references therein.

(5) (a) Masciocchi, N.; Cairati, P.; Ragaini, F.; Sironi, A. *Organometallics* **1993**, *12*, 4499. (b) Masciocchi, N.; Moret, M.; Cairati, P.; Ragaini, F.; Sironi, A. *J. Chem. Soc., Dalton Trans.* **1993**, 471.

(6) Baumgartner, M.; Schmalle, H.; Baerlocher, C. *J. Solid State Chem.* **1993**, *107*, 63.

0002-7863/94/1516-7668$04.50/0

prepared and characterized.[7b,8] Finally, a mixed-valence gold derivative, containing two Au(I) and one Au(III) metal centers *per* trinuclear unit, has been recently reported.[9]

In this paper we present the *ab-initio* crystal structure determination from powder diffraction data *only* of the α-$[Cu(pz)]_n$ (**1a**) and $[Ag(pz)]_n$ (**1b**) complexes (Hpz = pyrazole), which have been long known[10] but whose oligomeric or polymeric nature had never been clearly identified. A mixed metal $[(Cu,Ag)(pz)]_n$ phase **1c**, isostructural with **1a,b**, has also been prepared and its crystal structure successfully refined. In addition, the syntheses and the structures of the new β-$[Cu(pz)]_n$ (**2a**) and $[Ag(pz)]_3$ (**2b**) phases, which were unexpectedly obtained on modifying the syntheses of the **1a,b** phases, are also reported.

Experimental Section

Solvents were distilled and dried by standard methods. Pyrazole (Fluka), copper(I) oxide (Aldrich), and silver nitrate (Aldrich) were used as supplied. Tetrakis(acetonitrile)copper(I) tetrafluoroborate was prepared by following a procedure similar to that reported for the synthesis of $[Cu(CH_3CN)_4](PF_6)$[11] but employing aqueous HBF_4 instead of HPF_6. Elemental analyses were carried out at the Microanalytical Laboratory of this University. All complexes gave satisfactory analyses. IR spectra (Nujol mulls) were taken on a BIO-RAD FTS 7PC. DSC measurements were performed on a Perkin-Elmer DSC 7 instrument.

Synthesis of α-$[Cu(pz)]_n$ (1a). (a) To a solution of pyrazole (2.38 g, 35.0 mmol) in decaline (20 cm^3) maintained at 60 °C was added Cu_2O (0.50 g, 3.50 mmol). The temperature was raised to 150 °C and the suspension kept under stirring for 5 h. During this time a white precipitate formed. The temperature was then lowered to 60 °C and the solid filtered, washed with dichloromethane (20 cm^3) and acetone (50 cm^3), and dried *in vacuo* (0.90 g, >98% yield).

(b) To an acetone solution (35 cm^3) of pyrazole (1.50 g, 0.022 mol) was added $[Cu(CH_3CN)_4](BF_4)$ (3.46 g, 0.011 mol) under nitrogen. The colorless solution was stirred for 5 min, and then triethylamine (2.22 g, 0.022 mol) was added dropwise. A white precipitate suddenly formed. The suspension was stirred for 30 min and the solid filtered off, washed with acetone and CH_2Cl_2, and dried under vacuum (1.38 g, 96% yield). This synthetic method has been shown[12] to possess general validity and can be applied to a number of 3,5-substituted pyrazoles. α-$[Cu(pz)]_n$ can also be obtained by refluxing under nitrogen β-$[Cu(pz)]_n$ (*vide infra*) in 1,2-dichloroethane for 2 h.

Synthesis of $[Ag(pz)]_n$ (1b). The preparation of $[Ag(pz)]_n$ was originally reported by Buchner[13] and is here reported for completeness: NH_3 (25% water solution) was added to a solution of $AgNO_3$ (2.50 g, 14.7 mmol) in H_2O (40 cm^3) until the initially formed Ag_2O was completely dissolved, giving a clear solution. A water solution (30 cm^3) of pyrazole (7.50 g, 22.1 mmol) was then added dropwise. The white precipitate formed was filtered off, washed with water (50 cm^3) and methanol (50 cm^3), and dried under vacuum (2.54 g, >98% yield).

Synthesis of $[(Cu,Ag)(pz)]_n$ (1c). $[Cu(CH_3CN)_4](BF_4)$ (967 mg, 3.07 mmol) and $AgNO_3$ (522 mg, 3.07 mmol) were added, under nitrogen, to an acetonitrile solution (40 cm^3) of pyrazole (2.088 g, 0.031 mmol). The solution was kept under stirring for 5 min, and then triethylamine (1.25 g, 12.38 mmol) was added in a single portion. The white solid formed was filtered off, washed with CH_3CN and CH_2Cl_2, and dried under vacuum. Elemental analysis. Found: C, 23.26; H, 1.88; N, 18.02; Ag, 35.11. Calcd for $C_6H_6AgCuN_4$: C, 23.58; H, 1.96; N, 18.34; Ag, 35.33.

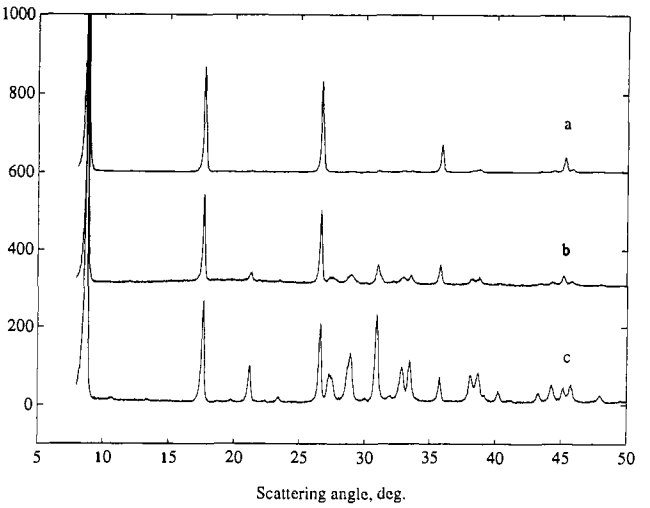

Figure 1. Effect of the sample preparation technique on the raw diffraction data of $[Ag(pz)]_n$: (a) deposition with 5% collodion in amyl acetate, (b) mixing arabic gum, and (c) side loading.

Synthesis of β-$[Cu(pz)]_n$ (2a). Cu_2O (0.540 g, 3.78 mmol) and pyrazole (5.14 g, 75.5 mmol) were heated in a sealed flask under nitrogen for 6 h at 150 °C without stirring. The mixture was then allowed to cool and solidify, giving a pale green solid. The residue was then washed with degassed dichloromethane (50 cm^3), that dissolves the small amount of copper(II) derivatives formed, and with acetone (20 cm^3) and finally filtered under nitrogen, giving 0.898 g (91% yield) of well-shaped colorless crystals.

Synthesis of $[Ag(pz)]_3$ (2b). Hydrogen peroxide (6 cm^3, 35% water solution) was added dropwise to a stirred dichloromethane solution (150 cm^3) of $[(PPh_3)Ag(pz)]_2$ (2.517 g, 2.88 mmol).[14] The white solid formed was then filtered off, washed with methanol (50 cm^3) and dichloromethane (50 cm^3), and dried under vacuum (0.849 g, 84% yield).

X-ray Structure Analysis. X-ray powder diffraction data were taken with Cu Kα radiation (λ = 1.5418 Å), on a Rigaku D-III MAX horizontal scan powder diffractometer equipped with parallel Soller slits, a graphite monochromator in the diffracted beam, a Na(Tl)I scintillation counter, and pulse height amplifier discrimination. The generator was operated at 40 kV and 40 mA. Slits used were DS (1.0°), AS (1.0°), and RS (0.3°).

The white powders were gently ground in an agat mortar, then cautiously deposited in an aluminum sample holder using the side-loading technique,[15] in order to minimize preferred orientation effects in the plane normal to the scattering vector. Several tests performed on the powders of the (isomorphous) **1a–c** phases showed that other specimen preparation techniques (*i.e* (i) the use of a binder, like 5% collodion in amyl acetate, and subsequent deposition of the viscous material onto a 511-oriented Si wafer or (ii) mixing arabic glue and the powdered sample followed by thorough milling of the resulting solid crust) resulted in extremely oriented powders with only a few measurable peaks attributable to what was later found to be 0*k*0 reflections (see Figure 1).

The final sets of data were collected, at room temperature, in the 5–85° (2θ) range, in the θ:2θ mode and step-scan with $\Delta 2\theta$ = 0.02° t = 10 s.

Standard peak search methods were used for location of the diffraction maxima, which were then fed to the trial and error indexing program TREOR.[16] All monometric and dimetric systems were unsuccessfully tested. A reasonable agreement for **1a** was found within the orthorhombic system, with a = 6.66 Å, b = 19.80 Å, c = 6.06 Å, $M(11)$[17] = 17, and $F(11)$[18] = 18 (0.013, 46). In the case of **1b**, TREOR found, among others, an orthorhombic unit cell of a = 6.51 Å, b = 20.02 Å, c = 6.45 Å, $M(10)$ = 38, and $F(10)$ = 33 (0.008, 40) which was reasonably similar to that of the copper derivative, therefore indicating the probable

(7) (a) Ehlert, M. K.; Rettig, S. J.; Storr, A.; Thompson, R. C.; Trotter, J. *Can. J. Chem.* **1990**, *68*, 1444. (b) Raptis, R. G.; Murray, H. H.; Fackler, J. P., Jr. *Inorg. Chem.* **1988**, *27*, 26. (c) Ehlert, M. K.; Storr, A.; Thompson, R. C. *Can. J. Chem.* **1992**, *70*, 1121. (d) Ehlert, M. K.; Rettig, S. J.; Storr, A.; Thompson, R. C.; Trotter, J. *Can. J. Chem.* **1989**, *67*, 1970. (e) Ehlert, M. K.; Rettig, S. J.; Storr, A.; Thompson, R. C.; Trotter, J. *Can. J. Chem.* **1991**, *69*, 432. (f) Ehlert, M. K.; Rettig, S. J.; Storr, A.; Thompson, R. C.; Trotter, J. *Can. J. Chem.* **1992**, *70*, 2161. (g) Bovio, B.; Bonati, F.; Banditelli, G. *Inorg. Chim. Acta* **1984**, *87*, 25.

(8) (a)Raptis, R. G.; Murray, H. H.; Fackler, J. P., Jr. *J. Chem. Soc., Chem. Commun.* **1987**, 737. (b) Raptis, R. G.; Fackler, J. P., Jr. *Inorg. Chem.* **1988**, *27*, 4179. (c) Ardizzoia, G. A.; Cenini, S.; La Monica, G.; Masciocchi, N.; Moret, M. *Inorg. Chem.* **1994**, *33*, 1458.

(9) Raptis, R. G.; Fackler, J. P., Jr. *Inorg. Chem.* **1990**, *29*, 5003.

(10) Trofimenko, S. *Chem. Rev.* **1972**, *72*, 497 and references therein.

(11) Kubas, G. J. *Inorg. Synth.* **1979**, *19*, 90.

(12) Ardizzoia, G. A.; La Monica, G. *Inorg. Synth.* **1994**, in press.

(13) Buchner, E. *Berichte* **1889**, *22*, 842.

(14) Ardizzoia, G. A.; La Monica, G.; Masciocchi, N.; Moret, M. Unpublished results.

(15) McMurdie, H. F.; Morris, M.; Evans, E.; Paretzkin, B.; Wong-Ng, W. *Powder Diffr.* **1986**, *1*, 40.

(16) Werner, P. E.; Eriksson, L.; Westdahl, M. *J. Appl. Crystallogr.* **1985**, *18*, 367.

(17) De Wolff, P. H. *J. Appl. Crystallogr.* **1968**, *1*, 108.

(18) Smith, G. S.; Snyder, R. L. *J. Appl. Crystallogr.* **1979**, *12*, 604.

Table 1. Crystal Data for α-[Cu(pz)]$_n$ (**1a**), [Ag(pz)]$_n$ (**1b**), [(Cu,Ag)(pz)]$_n$ (**1c**), β-[Cu(pz)]$_n$ (**2a**), and [Ag(pz)]$_3$ (**2b**)[a]

compound	1a	1b	1c	2a	2b
formula	$C_3H_3CuN_2$	$C_3H_3AgN_2$	$C_6H_6CuAgN_4$	$C_3H_3CuN_2$	$C_9H_9Ag_6N_6$
fw, amu	130.62	174.94	305.56	130.62	524.82
cryst syst	orthorhombic	orthorhombic	orthorhombic	orthorhombic	orthorhombic
space group	*Pbca*	*Pbca*	*Pbca*	*Pbcn*	*Pbcn*
a, Å	6.6684(4)	6.5295(4)	6.5765(4)	9.9332(15)	13.1469(14)
b, Å	19.8286(12)	20.0586(15)	20.0606(12)	13.3481(16)	10.5702(10)
c, Å	6.0847(4)	6.4675(4)	6.2743(4)	5.9538(8)	8.7921(9)
V, Å^3	804.6(1)	847.1(1)	827.8(1)	789.4(2)	1221.8(2)
Z	8	8	4	8	4
D_{calcd}, g cm^{-3}	2.156	2.743	2.451	2.206	2.853
T, °C	20	20	20	20	20
F(000)	512	656	584	512	984
no. of data points	3400	3400	3400	3400	3400
no. of reflections	558	592	575	559	924
2θ range, deg	17–85	17–85	17–85	17–85	17–85
R_p	0.033	0.086	0.042	0.036	0.115
R_{wp}	0.049	0.111	0.060	0.058	0.149
R_F	0.075	0.050	0.061	0.079	0.060
R_{Exp}	0.074	0.074	0.042	0.024	0.066
χ	0.7	1.5	1.4	2.4	2.3

[a] $R_p = \sum_i|y_{i,o} - y_{i,c}|/\sum_i|y_{i,o}|$; $R_{wp} = \sum_i w_i|y_{i,o} - y_{i,c}|^2/\sum_i w_i|y_{i,o}|^2$; $\chi^2 = \sum_i w_i|y_{i,o} - y_{i,c}|^2/(N_{obs} - N_{par})$; $R_{Exp} = R_{wp}/\chi$; and $R_F = \sum_k|F_{k,o} - F_{k,c}|/\sum_k|F_{k,o}|$, where $y_{i,o}$ and $y_{i,c}$ are the observed and calculated intensities, respectively, w_i is a statistical weighting factor (taken as $1/y_{i,o}$), and $F_{k,o}$ and $F_{k,c}$ are the observed and calculated structure factors; *i* runs over all data points and *k* runs over the space-group-permitted reflections. Note that, despite their rigorous statistical formulation (Prince, E. In *The Rietveld Method*; Young, R. A., Ed.; Oxford University Press: New York, 1993), the R_{Exp} and χ^2 values of Rietveld refinements heavily depend on the maximum intensity counts (Hill, R. J.; Madsen, I. C.; *Powder Diffr.* **1987**, *2*, 146) and, therefore, should be taken as *gross* goodness-of-fit indicators; on the contrary, the R_F index, although biased toward the calculated model during the partitioning procedure, is a more reliable indicator, since it depends more heavily on the fit of the crystal structure parameters and less on the nonstructural sources of misfit.

isomorphic nature of the two compounds. Density considerations lead to a *Z* value of 8 in both cases. Space group *Pbca* (no. 61) was chosen from systematic absences and subsequently confirmed by satisfactory refinement. Indexing of the mixed-metal [(Cu,Ag)(pz)]$_n$ powder spectrum afforded cell constants of approximate values 6.57 × 20.05 × 6.26 Å, intermediate between those of the copper and silver end members.

The solution of the structures of these three (isomorphous) phases was originally performed on the silver derivative, which, owing to the larger scattering power of this heavy atom, made the task of locating the unique crystallographically independent silver atom easier. The WPPF program[19] was used in order to extract the integrated intensities for 91 space group allowed reflections in the 5–55° range; these were then used in the scavenger-like program P-RISCON,[20] capable of setting an initial *rigid* model (here, the unique Ag atom) by refining the fractional coordinates of its center of mass and its angular orientation (not required in the case of a single atom). The minimum R_w value of 0.28 indicated that the silver atom had to be located approximately in 0.15, 0.50, 0.20. After the initial refinement of its location, performed with the standard DBW 3.2 program,[21] leading to R_p = 0.19, R_{wp} = 0.26, and R_{Bragg} = 0.13, simple packing and symmetry considerations indicated the location and orientation of the (bridging) pyrazolato groups. The same starting model was then assumed for the copper analogue.

Indexing of the [Ag(pz)]$_3$ phase gave a unit cell of *a* = 13.13, *b* = 10.56, and *c* = 8.79 Å [*M*(20) = 15, *F*(20) = 25 (0.012, 65)], indicating that 12 Ag(pz) formula units had to be present in the unit cell. Systematic absences indicated as probable space group *Pbcn* (no. 60), later confirmed by successful refinement. The program ALLHKL[22] was then used to extract integrated intensities, which were fed to the Direct Methods program SIRPOW.[23] It located two independent Ag atoms (one of which lying on a 2-fold axis) which allowed successful refinement down to R_p = 0.29 and R_{wp} = 0.37. The trimeric nature of the complex was then obvious, and the pyrazolate groups were added in ideal positions as a starting model.

For the sake of homogeneity, and in order to compare results from a similar experimental technique, powder diffraction data were also collected on thoroughly ground crystals of the copper β-phase and its structural parameters refined on these data, using prior knowledge from a single crystal X-ray determination.[24]

All structures were finally refined using the Rietveld technique and the GSAS package,[25] which allows the possibility of restraining geometrical parameters to known values. Only the data in the 17–85° (2θ) range were used, for which instrumental aberrations are minimized.[26] In the final runs, in order to stabilize the convergence of the refinements, all bond distances and angles within the pyrazolato groups were set at 1.38 Å and 108°, respectively, while the M–N distances were given soft restraints (and constrained to be equal); two sets of isotropic thermal parameters were used, one for the metals and the other for the lighter atoms. The contribution of the hydrogen atoms to the scattering factors was neglected.

Atomic scattering factors have been taken from the internal library of GSAS.[25] The background levels (relatively high in the copper derivatives, owing to fluorescent radiation) have been modeled using a six-term cosine Fourier series; the profile shape has been described by a pseudo-Voigt function[27] and an asymmetry parameter for the low-angle reflections accounting for the finite slit size.[25] The angular dependence of the full widths at half-maximum of the observed peaks was modeled following Caglioti *et al.*[28] for the Gaussian component, with GV set to zero,[25] while the Lorentzian broadening was refined as a strain (tan θ dependent) parameter.[29] The preferred orientation correction, in the formulation of Dollase and March,[30] was best effective if the 0*k*0 direction was selected. Final fractional atomic coordinates for compounds **1**–**c** and **2a**,**b** are given in the supplementary material. Crystal data and

(19) Toraya, H. *J. Appl. Crystallogr.* **1986**, *19*, 440.
(20) Masciocchi, N.; Bianchi, R.; Cairati, P.; Pilati, T.; Mezza, G.; Sironi, A. *J. Appl. Crystallogr.* **1994**, *27*, 426.
(21) Young, R. A.; Mackie, P. E.; Von Dreele, R. B. *J. Appl. Crystallogr.* **1977**, *10*, 262. Wiles, D. B.; Young, R. A. *J. Appl. Crystallogr.* **1981**, *14*, 149.
(22) Pawley, G. S. *J. Appl. Crystallogr.* **1981**, *14*, 357.
(23) Cascarano, G.; Favia, L.; Giacovazzo, C. *J. Appl. Crystallogr.* **1992**, *25*, 310.
(24) Ardizzoia, G. A.; LaMonica, G.; Masciocchi, N.; Moret, M. Paper presented at CO.GI.CO. '92 Camerino, Italy, p 25.
(25) Larson, A. C.; Von Dreele, R. B. *LANSCE, Ms-H805*; Los Alamos National Laboratory: New Mexico, 1990.
(26) With the X-ray optics used during our experiments, below 17°2θ, part of the X-ray flux is lost because the divergence of the primary beam results in a bathing section wider than the sample surface. Therefore, the integrated intensities of the few peaks lying in that region (1, 2, 2, 2, and 4 for **1a**, **1b**, **1c**, **2a**, and **2b**, respectively) are underestimated. In addition, the peak shapes are heavily affected, as vertical divergence effects (Klug, H. P.; Alexander, L. E. In *X-ray diffraction procedures for polycrystalline and Amorphous materials*; Wiley & Sons: New York, 1962; p 250), due to the finite size of the receiving slit, are very important at low θ angles, making any analytical correction troublesome. Therefore, while the presence of the low-angle peaks is of utmost importance in the process of deriving (i) the unit cell parameters and (ii) the starting structural model, it is common practice to leave them out in the final refinement procedures (ref 1, p 286). On including the few mentioned peaks in the refinements, R_p values are reaised to 0.07, 0.16, 0.10, 0.05, and 0.16 for **1a**, **1b**, **1c**, **2a**, and **2b**, respectively (see final R_p values in Table 1).
(27) Wertheim, G. K.; Butler, M. A.; West, K. W.; Buchanan, D. N. E. *Rev. Sci. Instrum.* **1974**, *45*, 1369.

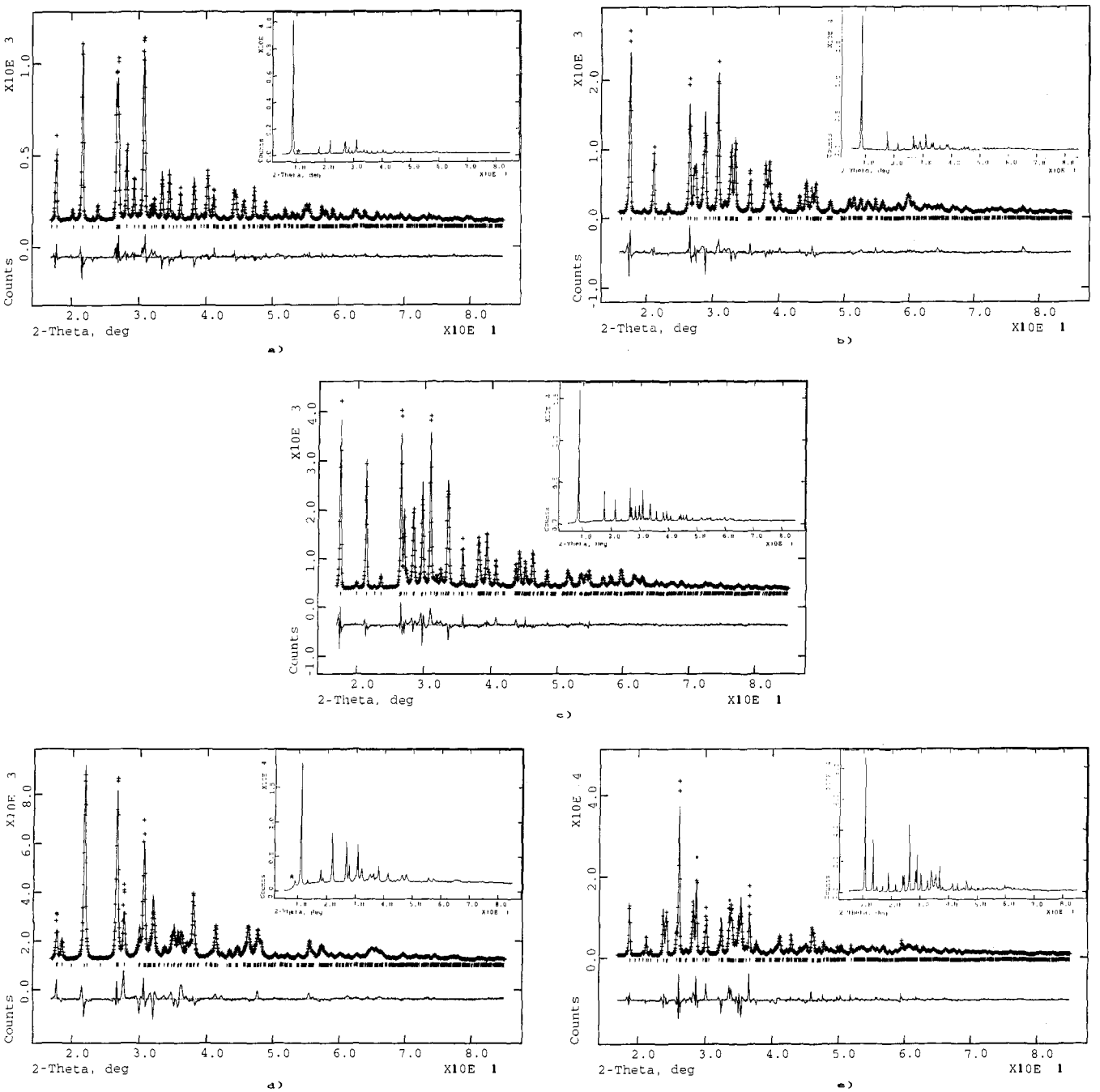

Figure 2. Plot of the observed (+) and calculated (solid) XRPD patterns in the 17-85° 2θ region (see the Experimental Section): (a) α-$[Cu(pz)]_n$, (b) $[Ag(pz)]_n$, (c) $[(Cu,Ag)(pz)]_n$, (d) β-$[Cu(pz)]_n$, and (e) $[Ag(pz)]_3$. Intensity scale in counts/s. Difference plots and the reflection markers are shown at the bottom. The inserts contain the raw data in the full 5–85° 2θ range; starred peaks arise from the mutual contamination of the two copper polymorphs.

final R_p, R_{wp}, and R_F values are reported in Table 1. Relevant bond distances and angles are collected in Table 2. Final plots of observed and calculated XRPD patterns are depicted in Figure 2a–e.

Results

Synthesis of α-$[Cu(pz)]_n$ (1a), $[Ag(pz)]_n$ (1b), and $[(Cu,Ag)(pz)]_n$ (1c). The reaction of $[Cu(CH_3CN)_4](BF_4)$ with pyrazole in acetone in the presence of triethylamine leads to the isolation of the α phase of $[Cu(pz)]_n$:

$$[Cu(CH_3CN)_4](BF_4) + Hpz \xrightarrow{Et_3N} (^1/_n)\alpha\text{-}[Cu(pz)]_n + (Et_3NH)BF_4 + 4CH_3CN \quad (1)$$
(1a)

Table 2. Relevant Bond Distances (Å) and Angles (deg) for α-$[Cu(pz)]_n$ (**1a**), $[Ag(pz)]_n$ (**1b**), $[(Cu,Ag)(pz)]_n$ (**1c**), and β-$[Cu(pz)]_n$ (**2a**)

compound	1a	1b	1c	2a
M···M *intra*chain	3.1653(6)	3.4034(4)	3.2894(5)	3.1453(2)
M···M *inter*chain	3.3373(2)	3.2731(2)	3.2934(2)	2.972(6)
M–N1[a]	1.86	1.97	1.91	1.86
M–N2[a]	1.86	1.97	1.91	1.86
N–M–N	166.6(1)	165.6(2)	173.6(2)	174(1), 158(1)
M···M···M *intra*chain	148.0(1)	143.7(1)	145.0(1)	142.3(2)

[a] Restrained M–N values (see the Experimental Section).

This preparation method works well not only for this particular compound but also for other copper(I) pyrazolato complexes, quantitative yields being obtained in all cases.[12] We have verified

that this synthetic route gives copper(I) pyrazolates whose nuclearity is related to the pyrazole employed. For example, 3,5-diphenylpyrazole (Hdppz) led to the isolation of the tetrameric complex $[Cu(dppz)]_4$, whose crystal structure has been recently reported.[8c]

$[Ag(pz)]_n$ (**1b**) has been quantitatively obtained by using the synthetic procedure originally reported more than 100 years ago by Buchner:[13]

$$AgNO_3 + Hpz \xrightarrow{NH_3\,(aq)} (^1/_n)[Ag(pz)]_n + NH_4NO_3 \quad (2)$$
$$(\mathbf{1b})$$

The close structural analogy between **1a,b** (see later) is probably related to the strict similarity of their preparation methods. Interestingly, the formation of a mixed-metal phase $[(Cu,Ag)(pz)]_n$ (**1c**) is observed when pyrazole is allowed to react with equimolar amounts of $[Cu(CH_3CH)_4](BF_4)$ and $AgNO_3$ in acetonitrile and, in order to avoid fractional precipitation phenomena, the deprotonating agent Et_3N is added in a single portion.

Synthesis of β-$[Cu(pz)]_n$ (2a) and $[Ag(pz)]_3$ (2b). The synthesis of β-$[Cu(pz)]_n$ is somewhat derived from the method described by Ehlert *et al.*[7a] for the preparation of $[Cu(dmpz)]_3$ (Hdmpz = 3,5-dimethylpyrazole). β-$[Cu(pz)]_n$ was obtained *via* a high-yield, high-temperature reaction of Cu_2O with molten pyrazole:

$$Cu_2O + 2Hpz \xrightarrow{150\,^\circ C} (^2/_n)\beta\text{-}[Cu(pz)]_n + H_2O \quad (3)$$
$$(\mathbf{2a})$$

We tried to extend this method to Ag_2O, with the aim of verifying the possible existence of a silver(I) pyrazolate phase different from **1b**. Our efforts failed owing to the high instability, under these experimental conditions, of the Ag_2O/pyrazole system due to the well-known oxidative properties of Ag_2O.

Nevertheless, a silver(I) pyrazolate phase quite different from **1b** was obtained by removing PPh_3 from the new dimeric silver(I) pyrazolato complex $[(PPh_3)Ag(pz)]_2$:[14]

$$3[(PPh_3)Ag(pz)]_2 \xrightarrow{H_2O_2} 2[Ag(pz)]_3 + 6O{=}PPh_3 \quad (4)$$
$$(\mathbf{2b})$$

This represents an interesting high-yield synthesis of a new silver(I) pyrazolate. Since $[Ag(pz)]_n$ and $[Ag(pz)]_3$ have substantial structural differences, one can expect to find also different chemical behaviors. In order to verify this assumption, we are presently studying their reactivity with nucleophiles (*e.g.*, phosphines), heterocumulenes (CO_2, COS, and CS_2), and olefines.

Figure 3 reports the IR spectra of complexes **1a–2b** in the 1300-600-cm^{-1} region. One can observe that the IR spectra are diagnostic for the identification of each phase. As expected, marked differences are present in the IR spectra of $[Ag(pz)]_n$ (**1b**) and $[Ag(pz)]_3$ (**2b**), owing to their different structural complexity. As a matter of fact, even the two copper(I) phases, **1a** and **2a**, can be distinguished by means of the different features of the IR absorptions in the 800-700-cm^{-1} region (764 and 741 cm^{-1} for **1a** and 758 and 735 cm^{-1} for **2a**). Finally, in agreement with the structural isomorphism, α-$[Cu(pz)]_n$ (**1a**) and $[Ag(pz)]_n$ (**1b**) exhibit very similar IR features. Nevertheless, the two species can be easily distinguished by the different patterns they exhibit in the 600-200-cm^{-1} region, as firstly reported by Okkersen *et al.*[31]

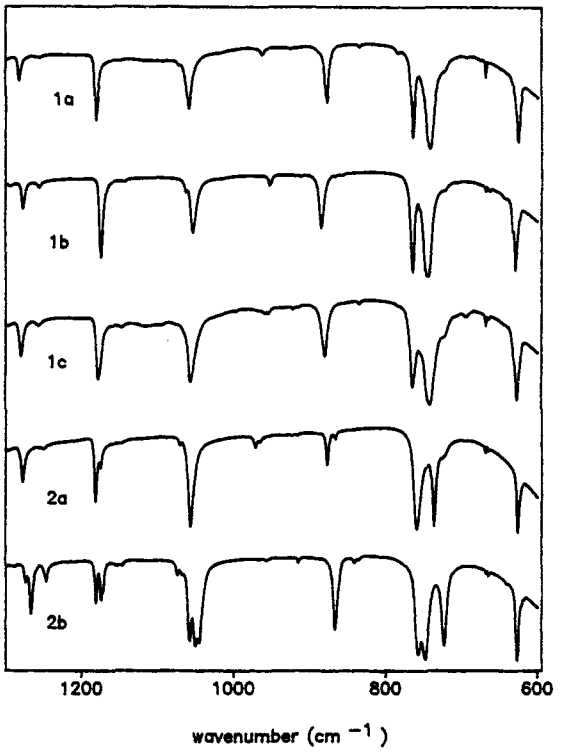

Figure 3. Infrared spectra (Nujol mulls) of α-$[Cu(pz)]_n$ (**1a**), $[Ag(pz)]_n$ (**1b**), $[(Cu,Ag)(pz)]_n$ (**1c**), β-$[Cu(pz)]_n$ (**2a**), and $[Ag(pz)]_3$ (**2b**).

Temperature- and Pressure-Induced Phase Transitions. Differential scanning calorimetry, performed under nitrogen flux (20 deg/min^{-1}), showed that α-$[Cu(pz)]_n$ is thermally stable up to 315 °C, where melting begins. Repeated thermal cycling of α-$[Cu(pz)]_n$ between room temperature and 275° resulted in completely unmodified powders and superimposable DSC traces. On the contrary, β-$[Cu(pz)]_n$, when heated in nitrogen atmosphere, showed a small endothermic peak, accounting for about 0.2 kcal mol^{-1}, at about 280 °C, which we interpreted as the β to α transformation on the basis of XRPD measurement of the heated sample. The same transformation occurs at much lower temperatures if 1,2-dichloroethane is used as a heating agent (see the Experimental Section), demonstrating that its presence is by far *noninnocent*, as it probably dissolves little quantities of β-$[Cu(pz)]_n$ which recrystallize then as the α phase. Of the two copper(I) phases, β-$[Cu(pz)]_n$, possessing a higher density, is likely to be stable at very low temperatures, while α-$[Cu(pz)]_n$, possessing a higher (less negative) heat of formation (as evidenced from the DSC trace), is stabilized at higher temperatures by entropic effects (*i.e.*, as later discussed, by the loosening of the Cu···Cu interchain interactions). The reverse $\alpha \rightarrow \beta$ transformation, which was never observed during our chemical experiments, was however achieved on pressing an α-$[Cu(pz)]_n$ pellet with 2 GPa for 14 h. The resulting material showed complete X-ray powder pattern identity with that of the β phase. Therefore, on using the proper technique, the α-$[Cu(pz)]_n$ and β-$[Cu(pz)]_n$ phases, which, owing to the high activation energy of the interconversion process, are indefinitely stable at room temperature, can be easily and 100% transformed from one into the other.

DSC measurements of $[Ag(pz)]_n$ and $[(Cu,Ag)(pz)]_n$, instead, showed exothermal decomposition at about 270 and 260 °C, respectively, as also evidenced by the dramatic blackening of the powders. We attribute this behavior (*i.e.*, the relative instability of these two polymers, if compared to their copper analogue, the α-$[Cu(pz)]_n$ phase) to the presence of the silver ions, which are well-known to be reduced to the metal by light exposure or moderate heating.

(28) Caglioti, G.; Paoletti, A.; Ricci, F. P. *Nucl. Instrum.* **1958**, *3*, 223.
(29) Thompson, P.; Cox, D. E.; Hastings, J. B. *J. Appl. Crystallogr.* **1987**, *20*, 79.
(30) Dollase, W. A. *J. Appl. Crystallogr.* **1987**, *19*, 267. March, A. *Z. Kristallogr.* **1932**, *81*, 285.
(31) Okkersen, H.; Groeneveld, W. L.; Reedijk, J. *Recl. Trav. Chim. Pays-Bas* **1973**, *92*, 945.

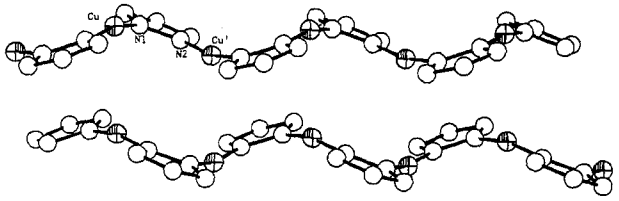

Figure 4. ORTEP drawing of two adjacent α-[Cu(pz)]$_n$ chains. At the drawing resolution, β-[Cu(pz)]$_n$ chains look similar.

Description of the Structures. α-[Cu(pz)]$_n$ and [Ag(pz)]$_n$ are isomorphous and isostructural compounds, consisting of infinite chains of M–pyrazolate (M = Cu, Ag) monomers, with the pyrazolato anions bridging symmetry-related metal ions. Each metal atom is approximately linearly coordinated (N1–Cu–N2 (166.6(1)°) and N1–Ag–N2 (165.5(1)°)) by two bridging pyrazolato groups, thus forming zig-zagged chains throughout the crystals, running along the crystallographic *c* axes and generated by the screw axis running parallel to *c*. An ORTEP drawing of the α-[Cu(pz)]$_n$ polymer is shown in Figure 4. The sequence of the metal atoms within each chain is not linear, but rather shows a folded shape, with M···M···M angles of about 148° and 144° for the Cu and Ag derivatives, respectively. This is due, at least in part, to the not coplanar nature of adjacent pyrazolates, which, in order to avoid short nonbonding H···H interactions, bend off and rather choose a folded ribbon conformation. The *intrachain* (pyrazolato bridged) M···M distances are 3.17 in **1a** and 3.40 Å in **1b**. In both compounds, the polymeric chains stack along (100), so that short *inter*molecular contacts between metal atoms of different chains are observed (Cu···Cu (3.337 Å) and Ag···Ag (3.273 Å)). Summarizing, owing to the space group symmetry of these polymeric phases, each metal atom experiences *two* short *intra*molecular and *two* short *inter*molecular contacts each, all well below 3.5 Å (see above).

The mixed-metal [(Cu,Ag)(pz)]$_n$ (**1c**) phase was found to be highly crystalline, with lattice parameters intermediate between those of the pure Cu and Ag members. The absence of extra (*Pbca* forbidden or supercell) reflections and the position of the peaks in the XRPD patterns clearly rule out any *ordered* Cu/Ag sequence in the polymeric chain or the presence of a mechanical mixture of α-[Cu(pz)]$_n$ and [Ag(pz)]$_n$. Thus [(Cu,Ag)(pz)]$_n$ is likely to be correctly formulated as a random copolymer (*solid solution*) of the Cu(pz) and Ag(pz) monomers, obtained under kinetic control during the fast precipitation from its solutions.

The β-[Cu(pz)]$_n$ form also contains folded polymeric ribbons, similar to those found in the α phase, with most of the *intra*molecular (*i.e.*, conformational) parameters unchanged. However, in the different packing environment of the β phase, which, formally, contains *dimers* of polymeric chains, with the *intra*dimeric Cu···Cu contact much shorter (2.972 vs 3.145 Å) than that within each chain, *all* other *inter*molecular M···M contacts are above 6 Å.

The structural relation between the α and β phases can be understood with reference to Figure 5 and Table 1; strict geometrical transformations exist between the observed cell parameters, *i.e.* $b(\beta) = 2a(\alpha)$ and $b(\alpha) = 2\alpha(\beta)$, making the *ab* products identical (in spite of the different assembling of the chains in the *ab* planes, as later discussed); as a consequence, the $c(\alpha)/c(\beta)$ and $V(\alpha)/V(\beta)$ ratios also agree (1.02); this shows that the different volumes of the two phases are mainly accounted for by the different stretching of the polymeric chains, as also partially evidenced by the values of the *intra*chain (pyrazolato bridged) Cu···Cu distances (see Table 3).

However, major stereochemical changes, evidenced in Figure 5, occur in the *ab* planes. In both compounds, the crystals can be ideally built by taking slabs (one molecular chain, *i.e.* about 3.3 Å thick) stacked normally to the *a* and *b* axes, in the α and β phases, respectively. Stacking of identical slabs along *a* (in the ...A*A*A*A*... sequence, italicized characters indicating a $c/2$ translation) generates a primitive rectangular packing (6.6 × 9.9 Å) of the polymeric chains in the α phase[32] (see Figure 5a). In the β phase, the sequence of the slabs is ..A*AB*B*A*A*BB*A*A*..., where B is a layer shifted by the $^1/_2(a + c)$ vector. In this case *b* represents a four-layer periodicity (..*AB*B*A*..). Two adjacent slabs (A*A* or B*B*) with short Cu···Cu contacts (<3 Å) contain, therefore, the dimeric units previously discussed; the crystal packing can therefore be interpreted as a pseudohexagonal array of dimers, as evidenced in Figure 5b.

In contrast with the three polymeric structures reported above, [Ag(pz)]$_3$ is a truly molecular compound whose topology closely resembles those of the already reported [Cu(dmpz)]$_3$ (Hdmpz = 3,5-dimethylpyrazole)[7a] and [M(dppz)]$_3$ (M = Cu, Ag, Au; Hdppz = 3,5-diphenylpyrazole)[8] trimers. An ORTEP drawing of the [Ag(pz)]$_3$ molecules is reported in Figure 6. The molecule lies, in the *Pbcn* space group, about a crystallographic 2-fold

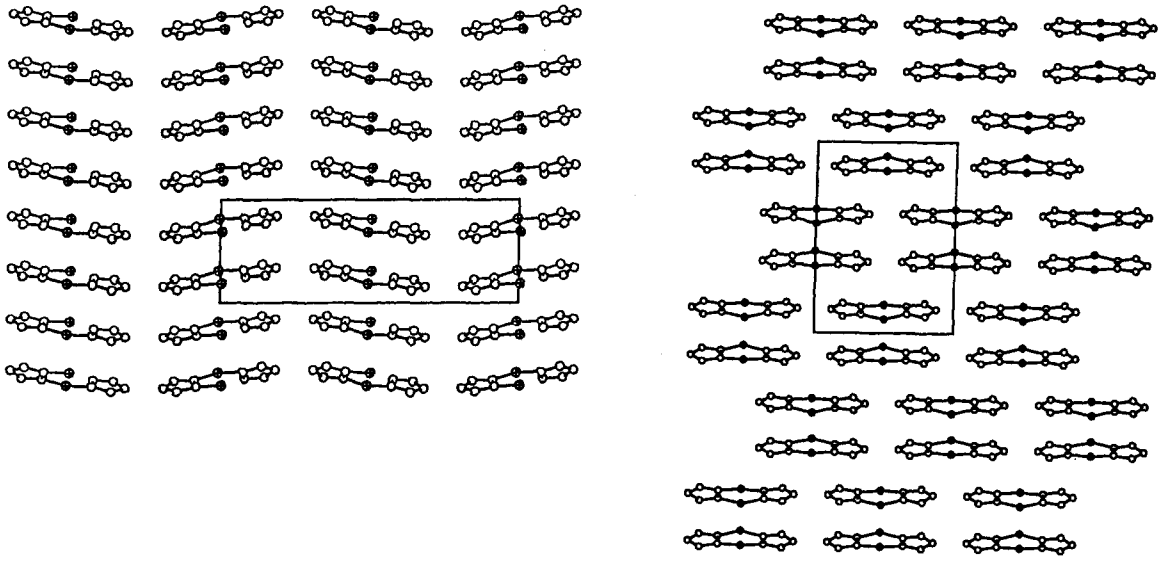

a) b)

Figure 5. Crystal packing (001 projection) of the (a) α-[Cu(pz)]$_n$ and (b) β-[Cu(pz)]$_n$ phases, showing the relative positions of the polymeric chains and their (a) *pseudo*rectangular and (b) *pseudo*hexagonal packing of chains and dimers, respectively.

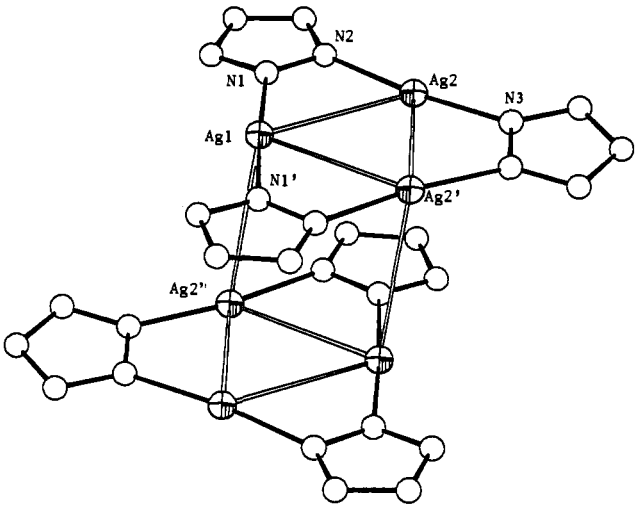

Figure 6. ORTEP drawing of the trimeric $[Ag(pz)]_3$ molecule. Two adjacent units are shown. Relevant bond distances (Å) and angles (deg) are as follows: Ag1–Ag2, 3.414(6); Ag2–Ag2′, 3.449(6); Ag1–N1, 2.24-(2); Ag2–N2, 2.23(2); Ag2–N3, 2.13(2); N1–Ag1–N1′, 177(1); N2–Ag2–N3, 172.1(7); Ag2–Ag1–Ag2′, 60.7(2); Ag1–Ag2–Ag2′, 69.7(5); Ag1–Ag2″ (*inter*trimer), 3.431(4).

axis but possesses idealized D_{3h} symmetry: it consists of an almost regular triangle of nonbonded Ag atoms (Ag1···Ag2(3,414(5) Å) and Ag2···Ag2′(3.431(4) Å)) whose sides are bridged by pyrazolato groups, in plane with the metals. Derived Ag–N bond distances are Ag1–N1(2.24(2) Å), Ag2–N2(2.23(2) Å), and Ag2–N3(2.13(2) Å); bond angles at the metals are N1–Ag1–N1′-(177(1)°) and N2–Ag2–N3(172.1(7)°). The significant twist of the pyrazolato coordination present in $[Ag(dppz)]_3$, but not in $[Au(dppz)]_3$ nor in $[Cu(dmpz)]_3$, is absent in the present compound. Similarly to what is described above for the β-$[Cu-(pz)]_n$ phase, $[Ag(pz)]_3$ also shows *inter*molecular metal–metal contacts comparable to those within each molecule (3.43 Å for the Ag1···Ag2 interaction between different trimers); they refer to short packing distances between adjacent molecules which are symmetry related by inversion centers. A similar arrangement of metal pyrazolato trimers facing their symmetry equivalents with short contacts has already been reported for $[Cu(dmpz)]_3$,[7a] where *inter*molecular contacts were found to be as low as 2.95 Å.

Discussion

Pyrazolato groups are well-known to be ideal *exo*-bidentate ligands capable of maintaining in close proximity, *i.e.* at distances typically around 3 Å, the metals to which they are attached. This is often a strict requirement for all those complexes possessing mutli-metal-centered catalytical activity, in a variety of different reactions, ranging from substrate oxidation by molecular dioxygen to hydrogenation of olefins.[33] In many known cases, however, the active molecules possess not only bridging pyrazolato groups but also other ligands which allow fine tuning of the catalytic activity and improve the stability and the solubility of the (otherwise unsoluble) binary metal pyrazolates.[33] Despite the rigid nature of the pyrazolato ring itself, a number of different coordination modes and conformations have been found in the literature; for example, (i) monodentate and *endo*-bidentate pyrazolato groups (although rare) have been structurally characterized,[34] (ii) six-membered rings generated by two *exo*-bidentate pyrazolates bridging two common metal atoms have been usually found as planar or boat conformers, but rare cases exhibiting a rather unusual and unexpected chair conformation have been recently reported,[8c] and (iii) oligomers of different nuclearity have been synthesized.[7b,8]

Table 3. List of Structurally Characterized Cu(I), Ag(I), and Au(I) Binary Pyrazolates and of Their Relevant Intermetallic Distances.

	Cu	Ag	Au
Hpz	α-$[Cu(pz)]_n$[a] **3.16**; 3.34, [*..tt..*] β-$[Cu(pz)]_n$[a] **3.14**; 2.97, [*..tt..*]	$[Ag(pz)]_n$[a] 3.27; **3.40**, [*..tt..*] $[Ag(pz)]_3$[a] **3.41**; 3.43; **3.44**, [*..tt..*] $[(Cu,Ag)(pz)]_n$[a] **3.29**; 3.29, [*..tt..*]	
Hdmpz	$[Cu(dmpz)]_3$[b] 2.95; **3.22**, [*ccc*]		
Hdppz	$[Cu(dppz)]_3$[c] **3.34**, [*ccc*] $[Cu(dppz)]_4$[e] **3.12**, [*ssss*]	$[Ag(dppz)]_3$[d] **3.39**, [*ccc*]	$[Au(dppz)]_3$[d] **3.37**, [*ccc*] $[Au(dppz)]_6$[f] **3.15–3.68**, [*cctcct*]
Htmpz	$[Cu(tmpz)]_3$[g] **3.07**, [*ccc*]		
Hdfmpz			$[Au(dfmpz)]_3$[h] **3.35**, [*ccc*]

[a] This work. Hpz = pyrazole, Hdmpz = 3,5-dimethylpyrazole, Hdppz = 3,5-diphenylpyrazole, Htmpz = 3,4,5-trimethylpyrazole, and Hdfmpz = 3,5-bis(trifluoromethyl)pyrazole. Values in bold characters refer to pyrazolato-bridged interactions. [b] Reference 7a. [c] Reference 8b. [d] Reference 7b. [e] Reference 8c. [f] Reference 8a. [g] Reference 7f. [h] Reference 7g.

A simple geometrical model for the pyrazolato groups bound to group 11 metal atoms, allowing the nature, conformation, and stoichiometry of all known binary metal pyrazolates reported in Table 3 to be foreseen, can be based on the following assumptions:

(1) All pyrazolato ligands must bind in the (most common) *exo*-bidentate fashion.

(2) In keeping with the electronic requirements of linearly coordinated M(I) atoms (M = Cu, Ag, Au), the N–M–N angles should not deviate heavily from 180°.

(3) The metal atoms should lie more or less in the plane of each adjacent pyrazolate and give N–N–M angles of about 126°.

(4) Accordingly to what is sketched in Figure 7, the dihedral angles between pyrazolato ligands bound to a metal atom are not constrained to specific values but can range from 0° (*cis* conformation) up to 180° (*trans* conformation); an intermediate value of 90° is hereafter referred to as the *staggered* conformation.

Therefore, *all* binary 1:1 metal pyrazolates of this class can be described by *n* characters (*n* being the nuclearity of the molecule) referring to the idealized conformation types about each metal atom; for example, the *cis–cis–cis* arrangement of pyrazolato ligands in $[Ag(pz)]_3$, as well as those of the other trimers $[Cu(dmpz)]_3$, $[Cu(dppz)]_3$, $[Ag(dppz)]_3$ and $[Au(dppz)]_3$, can be referred to by [*ccc*]. Accordingly, the same conformational analysis gives for $[Cu(dppz)]_4$ a [*ssss*] and for $[Au(dppz)]_6$ a [*cctcct*] symbol. Within this system, also, the three new polymers presented in this paper can be labeled as cycles of infinite length in the *new all-trans* [*..tt..*] conformation. It should be noted, however, that a cyclic *all-trans* pyrazolato fragment, possessing eight metal centers, is indeed already known: it can be formally obtained by removing the eight hydroxyl groups from the recently characterized octameric $[Cu_8(dmpz)_8(OH)_8]$ molecule.[35]

The extreme variety observed in the nuclearities and stoichiometries of copper, silver, and gold pyrazolates is accompanied

(32) The observed doubling of its *b* axis must be ascribed to the nonequivalence of adjacent molecules within each slab, which are neither strictly planar nor equally tilted.

(33) Estervelas, M. A.; Garcia, M. P.; Lopez, A. M.; Oro, L. A. *Organometallics* **1991**, *10*, 127.

(34) Bandini, A. L.; Banditelli, G.; Bonati, F.; Minghetti, G.; Demartin, F.; Manassero, M.; *J. Organomet. Chem.* **1984**, *269*, 91. Bovio, B.; Bonati, F.; Banditelli, G. *Gazz. Chim. Ital.* **1985**, *115*, 613. Eigenbrot, C. W.; Jr.; Raymond, K. N. *Inorg. Chem.* **1982**, *21*, 2653.

(35) Ardizzoia, G. A.; Angaroni, M. A.; La Monica, G.; Cariati, F.; Moret, M.; Masciocchi, N.; *J. Chem. Soc., Chem. Commun.* **1990**, 1021. Ardizzoia, G. A.; Angaroni, M. A.; La Monica, G.; Cariati, F.; Cenini, S.; Moret, M.; Masciocchi, N. *Inorg. Chem.* **1991**, *30*, 4347.

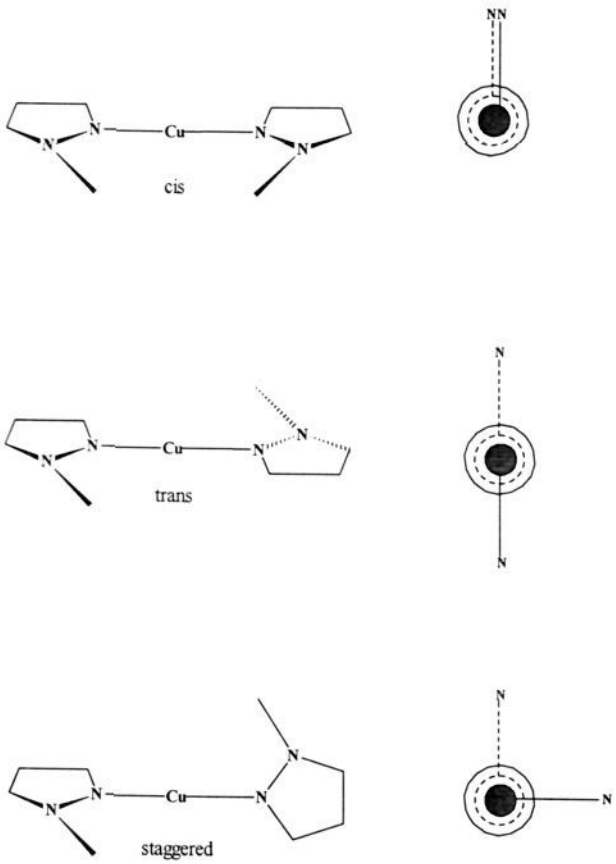

Figure 7. Schematic drawing of (a) *trans*, (b) *cis*, and (c) *staggered* pz–M–pz (pz = pyrazolato) linkages.

by the possibility of stacking moieties of similar size and shape (here, the $[Cu(pz)]_n$ ribbons) into different space groups and, therefore, different packing environments. There is, however, a rationale for this behavior: many structural features observed for group 11 pyrazolates can be found in the realm of purely organic pyrazoles, where hydrogen bonding between different molecules is capable of generating, in the solid state, a variety of Hpz* clusters, ranging from dimers up to polymeric chains.[36] This analogy goes even further, as it can be observed that a fairly straight parallelism between pure and Cu(I)-substituted pyrazoles exists: pyrazole[36a,b] (Hpz) and $[Cu(pz)]_n$ (α and β phases) are polymeric (although of different helical conformations) and 3,5-dimethylpyrazole[36c,d] (Hdmpz) and $[Cu(dmpz)]_3$ are (D_{3h}) trimers, while 3,5-diphenylpyrazole[36g] (Hdppz) and the recently characterized $[Cu(dmpz)]_4$ molecules are tetramers of (idealized) D_{2d} symmetry. This, in turn, might suggest that the (static)

(36) (a) Berthou, J.; Elguero, J.; Rerat, C. *Acta Crystallogr.* **1970**, *B26*, 1880. (b) Krebs, Larsen, F.; Lehmann, M. S.; Sotofte, I.; Rasmussen, S. E. *Acta Chem. Scand.* **1970**, *24*, 3248. (c) Baldy, A.; Elguero, J.; Faure, R.; Pierrot, M.; Vincent, E. J. *J. Am. Chem. Soc.* **1985**, *107*, 5290. (d) Smith, J. A. S.; Wehrle, B.; Aguilar-Parrilla, F.; Limbach, H. H.; Foces-Foces, M.; Cano, F. H.; Elguero, J.; Baldy, A.; Pierrot, M.; Khursid, M. M. T.; Larcombe-McDouall, J. B.; *J. Am. Chem. Soc.* **1989**, *111*, 7304. (e) Maslen, E. N.; Cannon, J. R.; White, A. H.; Willis, A. C. *J. Chem. Soc., Perkin Trans.* **1974**, 1298. (f) Moore, F. H.; White, A. H.; Willis, A. C.; *J. Chem. Soc., Perkin Trans.* **1975**, 1068. (g) Aguilar-Parrilla, F.; Scherer, G.; Limbach, H. H.; Foces-Foces, M.; Cano, F. H.; Smith, J. A. S.; Toiron, C.; Elguero, J. *J. Am. Chem. Soc.* **1992**, *114*, 9657. (h) Aguilar-Parrilla, F.; Cativiela, C.; Diaz de Villegas, M. D.; Elguero, J.; Foces-Foces, C.; Garcia Laureiro, J. I.; Cano, F. H.; Limbach, H. H.; Smith, J. A. S.; Toiron, C.; *J. Chem. Soc., Perkin Trans.* **1992**, 1737. (i) Foces-Foces, C.; Cano, F. H.; Elguero, J.; *Gazz. Chim. Ital.* **1993**, *123*, 477. (j) Llamas-Saiz, A. L.; Foces-Foces, C.; Sobrados, I.; Elguero, J.; Meutermans, W. *Acta Crystallogr.* **1993**, *C49*, 724. (k) Raptis, R. G.; Staples, R. J.; King, C.; Fackler, J. P., Jr. *Acta Crystallogr.* **1993**, *C49*, 1716.

Table 4. Partitioning of the MM Steric Energies (kcal mol^{-1}) for Polymeric Cu(I) and Ag(I) Pyrazolates

	α-$[Cu(pz)]_n$	β-$[Cu(pz)]_n$	α-$[Ag(pz)]_n$	β-$[Ag(pz)]_n$
*intra*molecular	+2.03	+2.63	+1.51	+2.09
vdW (chain)	*–0.65*	*–0.98*	*–0.37*	*–0.59*
charges (chain)	–0.22	–0.22	–0.22	–0.22
vdW (packing of chains)	–5.21	–5.19	–4.88	–4.93
charges (packing of chains)	+0.29	–0.05	+0.29	–0.06
total	–3.76	–3.81	–3.67	–3.71

N–Cu–N (with a N···N distance of about 3.7 Å) and (dynamic, thus tautomeric) N–H···N (with a N···N of about 2.9 Å) bonds, in spite of their different nature and strength, are (linear) hinges about which the pyrazolato rings are essentially free to rotate. The different steric demands of different substituents in the 3,5 positions of the heterocycles drive the preferred dihedral angle to specific values, thus determining the nuclearity of the oligomers and the size of the $[...N–N–X–..]_n$ (X = H, Cu) loops; the analogy of the linear coordination at the H^+ or Cu^+ acidic centers imposes local packing of the monomers but does not determine the supramolecular arrangement in the crystal, so that crystal systems and space groups of the H and Cu derivatives do not match. The existence of two polymeric $[Cu(pz)]_n$ phases and of the polymeric chain of pyrazole itself (which heavily differ from those of the copper analogues) confirms this observation. Again, Figure 5 nicely shows how the α and β copper pyrazolate phases heavily differ at a supramolecular level.

Interestingly, two molecules of remarkably different sizes, 3-methyl-5-phenylpyrazole[36e,f] and 3,5-diphenylpyrazole,[36f,k] pack in the same space group, with two independent molecules each, both located in proximity of the 2-fold axis, giving rise to tetramers whose intermolecular proton transfer has been evidenced, in the solid state, by neutron diffraction[36f] and, more recently, ^{15}N CP/MAS NMR.[36g] This allows us to predict, on a steric ground only, that the (still unknown) copper 3-methyl-5-phenylpyrazolate might be tetrameric as well. In contrast, the existence, in the solid state, of dimers of 4-bromo-3,5-diphenylpyrazole[36g] cannot be counterparted by a dimeric form of its copper derivative, which does not allow any (more or less) linear coordination at the metal.

We have recently modified the MM3 program[37] in order to deal with crystalline materials, even if polymeric.[38] We are presently able to refine the intramolecular degrees of freedom in the presence of the crystal lattice constraints. Thus, because the proposed geometrical model for the group 11 metal/pyrazolato system can be formulated using the language of molecular mechanics (force field parameters are supplied in the *supplementary material*), we have attempted to model the three polymeric α-$[Cu(pz)]_n$, β-$[Cu(pz)]_n$, and $[Ag(pz)]_n$ ("α-$[Ag(pz)]_n$") compounds and a hypothetical "β-$[Ag(pz)]_n$" phase, isomorphous with β-$[Cu(pz)]_n$, with lattice parameters (a = 10.0484, b = 13.0701, and c = 6.3284 Å) extrapolated from those of the three known phases.

Preliminary results (see Table 4) indicate that the α phases are substantially equienergetic to the corresponding β phases. Note, however, that we have not attempted to parametrize the M···M interactions, whose energy contribution should be hopefully small but, perhaps, not negligible. The quality of the force field and the small energy difference to be reporduced do not allow us to draw any definite conclusion on the subject, but on partitioning the different energetic effects, we found that α phases are favored by intramolecular interactions (stretching, bending, torsional, and 1,4 van der Waals) while β phases possess a better organization (i) of the monomers within each chain (favored by long-range van der Waals interactions) and (ii) of the chains in the crystal (favored by Coulombic forces). In other words, *intra-* and

(37) Allinger, N. L.; Yuh, Y. H.; Lii, J. H.; *J. Am. Chem. Soc.* **1989**, *111*, 8551.

(38) Moret, M.; Sironi, A. To be published.

*inter*molecular interactions do not cooperate, favoring the α and β phases, respectively.

Conclusions

The structural chemistry of group 11 binary pyrazolates shows a variety of stoichiometries and conformations for which a simple geometrical model has been proposed. In addition, the topological relationships within the metal pyrazolato moleculs and with the purely organic moieties have shown the relative importance of hydrogen bonds, metal–ligand interactions, and crystal packing forces in determining the assembly of the monomers.

We have shown that important structural features such as stoichiometry, conformation, and crystal packing of Cu(I) and Ag(I) pyrazolates, failing to afford single crystals of suitable size, can be determined by using conventional X-ray powder diffraction techniques. Owing to the intrinsic loss of information of powder data, if compared to the 3D sampling of the reciprocal space normally performed by single crystal techniques, only a limited number of structural parameters can be confidently refined; however, the inclusion of all chemical knowledge using restraints for *chemically equivalent* geometrical features can undoubtedly help in the refinement procedure.

Acknowledgment. The Italian CNR (Progetto Finalizzato Materiali e Tecnologie Avanzate and Progetto Finalizzato Chimica Fine II) is acknowledged for funding. The technial support of Mr. G. Mezza is also acknowledged.

Supplementary Material Available: Additional material available comprises lists of fractional atomic coordinates, full lists of bond distances and angles and force field parameters, and lists of reflection indexes, positions, and intensities (77 pages). This material is contained in many libraries on microfiche, immediately follows this article in the microfilm version of the journal, and can be ordered from the ACS; see any current masthead page for ordering information.